

014

~~CONFIDENTIAL~~ CONFIDENTIAL

Copy 6
RM E52E22

701 1952

~~CONFIDENTIAL~~



NACA RM E52E22

RESEARCH MEMORANDUM

CLASSIFICATION CANCELLED

Authority NACA Res. Obs. Date 3/14/56

RN 101
By Inst. A 6/1/56 See _____

DESIGN AND TEST OF MIXED-FLOW IMPELLERS

II - EXPERIMENTAL RESULTS, IMPELLERS

MODEL MFI-1A

By Joseph R. Withee, Jr., and William L. Bee

Lewis Flight Propulsion Laboratory
Cleveland, Ohio

CLASSIFICATION CHANGED

To: _____
By authority of R.F.M. Date 1/11/56
Inst. A 6/1/56

- 09/12/11 KJW

~~CONFIDENTIAL~~ C ~~CONFIDENTIAL~~ CANCELLED

Auth: _____ Date 10/21/54

By Inst. A 6/1/56 See _____

CLASSIFIED DOCUMENT

This material contains information affecting the National Defense of the United States within the meaning of the espionage laws, Title 18, U.S.C., Secs. 793 and 794, the transmission or revelation of which in any manner to unauthorized person is prohibited by law.

NATIONAL ADVISORY COMMITTEE FOR AERONAUTICS

WASHINGTON
September 19, 1952

~~CONFIDENTIAL~~

UNCLASSIFIED

CONFIDENTIAL

NACA LIBRARY
LANGLEY AERONAUTICAL LABORATORY
Langley Field, Va.

~~CONFIDENTIAL~~ UNCLASSIFIED

1B

NACA RM E52E22

~~CONFIDENTIAL~~



NATIONAL ADVISORY COMMITTEE FOR AERONAUTICS

RESEARCH MEMORANDUM

DESIGN AND TEST OF MIXED-FLOW IMPELLERS

II - EXPERIMENTAL RESULTS, IMPELLER

MODEL MFI-1A

By Joseph R. Withee, Jr., and William L. Beede

SUMMARY

An investigation was conducted to determine the performance characteristics of a mixed-flow impeller which was designed with special emphasis on the reduction or elimination of flow decelerations along the wetted surfaces. The blade height as designed for isentropic flow was increased considerably (74 percent at the outlet) so subsequent investigations could be made with reduced blade heights to obtain an estimate of the area allowance which should be made for viscous effects.

The performance was investigated over a range of equivalent impeller speeds from 700 to 1600 feet per second and over a range of flow rates from maximum to point of incipient surge. The peak pressure ratio and maximum adiabatic temperature-rise efficiency, measured at $1\frac{1}{2}$ impeller diameters in a vaneless diffuser, at the design speed of 1400 feet per second were 4.00 and 0.83, respectively. The efficiency over the greater part of the flow range at equivalent speeds from 900 feet per second to design speed (1400 ft/sec) was higher than 0.80. At design speed, the arbitrary increase in blade height near the impeller outlet was not too small to allow for the decrease in effective flow area caused by viscous effects. The ability of the impeller to pass 6 to 7 percent greater mass flow at design speed than was theoretically predicted was probably due to negative angles of attack, which increased the flow area at the inlet.

INTRODUCTION

A series of mixed-flow impellers is being designed and experimentally tested at the NACA Lewis laboratory. The aerodynamic design procedure for the first of these impellers, designated the MFI-1, is presented in reference 1. In the design, special emphasis was placed upon the reduction or elimination of flow decelerations along the wetted surfaces. It was found in the design analysis that the high relative velocities at the impeller inlet near the tip necessitated some decelerations on the blade surfaces near the shroud. However, it was believed that the

~~CONFIDENTIAL~~ ~~CONFIDENTIAL~~

UNCLASSIFIED

2567

reductions in decelerations which were effected, particularly along the trailing face of the blade and at the hub, would result in a relatively high over-all efficiency. The blade height of the MFI-1 impeller as originally designed for isentropic flow was increased considerably (74 percent at the outlet) to allow for viscous effects, which decrease the effective flow area, and to increase the ratio of blade height to passage width. Splitter blades were added to further increase the ratio of blade height to passage width. The increase in blade height also reduced the ratio of clearance space to blade height, which reduced the effect of air spillage through the clearance space between the impeller blades and the shroud. The theoretical analysis of the impeller with these modifications (MFI-1A) is also presented in reference 1. These modifications will be eliminated by successive reductions in the blade height and the removal of the splitter blades of the experimental impeller in order to obtain a better estimate of the allowances which should be made.

This report presents the performance characteristics of the modified impeller, designated the MFI-1A. The outlet tip diameter is 15.29 inches and the mean outlet angle in the hub-to-shroud (meridional) plane is 30° from the axis of rotation. The performance was investigated over a range of equivalent speeds from 700 to 1600 feet per second and over a range of flow rates from maximum to point of incipient surge. Incipient surge was taken as the point at which a slight decrease in weight flow would have caused audible surge. The performance is analyzed and compared with the theoretical analysis of the impeller designed for isentropic flow (MFI-1) as presented in reference 1. As the modifications were of an arbitrary nature, exact agreement between the theoretical analysis of reference 1 and the experimental analysis of this report was not anticipated.

SYMBOLS

The following symbols are used in this report:

- f_s slip factor, ratio of tangential velocity of air at impeller outlet to tangential velocity of blades at impeller outlet
- L ratio of distance from impeller inlet measured along surface of shroud to total length of shroud
- Q ratio of velocity relative to impeller to speed of sound for inlet stagnation conditions
- U actual impeller speed based on 7.00-in. radius, ft/sec
- W actual air-weight flow, lb/sec

- 2567
- δ ratio of inlet total pressure to NACA standard sea-level pressure (29.92 in. Hg abs)
- η_{ad} adiabatic temperature-rise efficiency
- θ ratio of inlet total temperature to NACA standard sea-level temperature (518.4° R)
- φ angle between projection of center line of blade-inlet radial section and projection of center line of any other blade radial section on plane perpendicular to axis of rotation, deg
- φ' angle between projection of center line of blade-inlet radial section and projection of radial line through driving face of splitter blade at hub on plane perpendicular to axis of rotation, deg

APPARATUS AND INSTRUMENTATION

Apparatus

The impeller used in this investigation was an aluminum-alloy impeller of the mixed-flow type with 21 complete blades and 21 splitter blades (fig. 1). The inlet tip diameter was 9.45 inches and the outlet tip diameter was 15.29 inches. This impeller had an inlet hub-tip ratio of 0.355, and an outlet hub-tip ratio of 0.878. The over-all axial length was 6.31 inches. At the outlet the blades were curved backward (relative tangential-velocity component opposite to wheel rotation) through an average angle of 8.7° (fig. 2). The mean outlet angle in the hub-to-shroud (meridional) plane was approximately 30° from the axis of rotation. Detailed design data for the MFI-1A and MFI-1 impellers are presented in table I. The variation of radial blade height of the two impellers is presented in figure 3.

The experimental setup is shown in figure 4. Air passed through a submerged adjustable orifice, through a filter tank, then into a stagnation chamber that housed the inlet instrumentation. From the stagnation chamber, the air passed through a converging inlet, the impeller, a vaneless diffuser, and into a collector; it was then discharged into the laboratory exhaust system. The vaneless-diffuser area was reduced to 95 percent of the diffuser-inlet area in the first inch of length and was maintained constant at 95 percent thereafter.

Instrumentation

The weight flow through the compressor was measured by means of a submerged adjustable orifice. Temperatures were measured by use of thermocouples in conjunction with a calibrated potentiometer. All pressures were measured by use of water or mercury manometers. In this investigation, calibrated bare-wire spike-type thermocouples and Kiel type total-pressure probes were used (fig. 5). All static-pressure taps were 0.030 inch in diameter.

Over-all performance. - The location of the inlet measuring station is shown in figure 4. Six thermocouples and six total-pressure probes were located at the root-mean-square radii of three equal annular areas. These instruments, along with two wall static-pressure taps located on opposite sides of the stagnation chamber, were used to determine the state of the inlet air.

The outlet measuring station was located at a 10.5-inch radius ($1\frac{1}{2}$ -impeller outlet mean-line radii) as shown in figure 6. This location was selected on the basis of the data presented in reference 2. With the MFI-1A impeller, approximately 40 percent of the kinetic energy of the air is converted into static pressure, and it is estimated that most of the mixing losses are assimilated. The outlet instrumentation consisted of twelve total-pressure probes, eight static-pressure taps, and four thermocouple rakes distributed in a uniform pattern around the front and rear diffuser walls. The three thermocouples on each rake and the total-pressure probes were located at the centers of three equal areas across the diffuser passage which was 0.5 inch in width.

Analysis. - The location of the instrumentation used in obtaining data for a detailed analysis is shown in figure 6. A three-dimensional ball-type probe (fig. 5(a)), located approximately $\frac{3}{4}$ -inch upstream of the impeller leading edge, was used to measure the total pressure, static pressure, and air-flow angle in the circumferential and radial directions. A wedge-type static-pressure rake (fig. 5(b)) and a total-pressure rake were located at the leading edge of a nonrotating dummy hub which was used in mock-up tests to determine the effects of the hub and shroud curvatures upon the entering flow. Fifty-three static-pressure taps were distributed along the front shroud and the front and rear diffuser walls.

Precision of measurements. - The precision of the measurements is estimated to be within the following limits:

Pressure, in. Hg abs	±0.04
Temperature, °F	±2.0
Air weight flow, percent	±1.0
Speed, percent of design	±0.30

PROCEDURE AND COMPUTATIONS

Procedure

This investigation was carried out at a constant inlet air pressure of 14 inches of mercury absolute. Ambient air at 77° to 82° F was used at equivalent impeller speeds of 700 to 1400 feet per second. At 1600 feet per second, an inlet temperature of -39° F was chosen because of impeller stress considerations. The flow rate was varied from maximum to the point of incipient surge by varying the outlet pressure. Incipient surge was taken as the point at which a slight decrease in weight flow would have caused audible surge.

The equivalent impeller speed was varied from 700 to 1600 feet per second, based upon a radius of 7.00 inches rather than upon the actual impeller-outlet tip radius of 7.65 inches to enable comparison of the theoretical analysis of reference 1 and the experimental results of this report.

At impeller speeds of 900, 1100, and 1400 feet per second, with the impeller operating near the peak pressure ratio, a radial survey was made 3/4 inch upstream of the impeller inlet (fig. 6) by use of a ball-type three-dimensional probe. Surveys with the same probe were made at this location with corresponding equivalent weight flows and the dummy hub in position. In addition, with the dummy hub, measurements were made in the plane of the impeller inlet by means of total- and wedge-type static-pressure rakes. Limitations of the system restricted the maximum equivalent weight flow with the dummy hub to 12.0 pounds per second.

Computations

Adiabatic temperature-rise efficiency. - The inlet temperatures and pressures were computed from an arithmetic average of the temperatures and pressures measured in the stagnation chamber. Because of the large gradients in the temperature and pressure measurements across the diffuser passage, the outlet total temperatures and total pressures (at the 10.5-in. radius) were based upon a mass-flow average.

Angle of attack at impeller inlet. - Obviously, it was impossible to operate survey instruments in the plane of the impeller inlet with the impeller in operation so the axial-velocity profile used in computing the angle of attack at the inlet was determined as follows: The analysis of reference 1 indicates that the acceleration (or deceleration) in the

axial-flow component upstream of the impeller would be similar to that upstream of the dummy hub. Therefore, the acceleration in axial flow at each radial position for the dummy hub from 3/4 inch upstream of the inlet to the inlet was applied to the axial component of the velocity measured 3/4 inch upstream of the rotating impeller. At the design impeller speed, 1400 feet per second, the weight flow at the peak pressure ratio was greater than 12.0 pounds per second; therefore, the accelerations obtained at lower weight flows with the dummy hub were extrapolated to compute the angle of attack at that speed. The extrapolation made by plotting acceleration against equivalent weight flow resulted in a practically straight-line relation. The possible error introduced in the computed angle of attack by making the extrapolation is of the order of 1.

Slip factor. - The slip factor is based on an average inlet air temperature, mass-flow-average outlet temperature, and an actual impeller speed as computed at a root-mean-square radius of 7.19 inches, which is approximately the radius of the average flow.

Velocity relative to impeller. - Total pressures along the shroud were computed, in accordance with reference 3, from measured values of inlet air temperature, inlet air pressure, impeller speed, and a selected value of internal impeller efficiency, 0.90. From these total pressures and measured values of experimental static pressure, the mean velocity along the shroud relative to the impeller was computed (reference 3).

PERFORMANCE AND ANALYSIS

Over-All Performance

The experimental over-all performance characteristics of the MFI-1A impeller are shown in figure 7 for a range of equivalent impeller speeds from 700 to 1600 feet per second and a range of equivalent flow rates from maximum to point of incipient surge. Adiabatic temperature-rise efficiency for a range of equivalent speeds from 900 to 1600 feet per second is presented in figure 8. The efficiency at 700 feet per second is omitted because the temperature rise through the impeller was of such small magnitude that an inaccuracy of $\pm 2.0^\circ$ F in temperature measurements resulted in discrepancies of ± 0.025 in efficiency. The peak pressure ratio and the maximum adiabatic efficiency at the design equivalent speed, 1400 feet per second, were 4.00 and 0.83, respectively. The maximum efficiency (0.89) occurred at an equivalent speed of 900 feet per second and a pressure ratio of 1.98. The efficiency over the greater part of the flow range at equivalent speeds from 900 feet per second to design speed was higher than 0.80.

Analysis

Geometric coordinates for both the MFI-1 impeller and MFI-1A impeller are given in table I. For the MFI-1A impeller, the blade height was arbitrarily increased to allow for effective reduction in through-flow area due to viscous effects; therefore, it was expected that the closest agreement would be between the values obtained in the theoretical analysis of the MFI-1 impeller and the experimental results for the MFI-1A impeller. All comparisons in this analysis are made on that basis.

At the design equivalent speed of 1400 feet per second, the experimental weight flows of 14.3 and 13.4 pounds per second were closest to the weight flows used in the analysis of the MFI-1 impeller in reference 1 (14.5 and 13.0 pounds per second, respectively). Therefore, the results obtained at these two weight flows are used in the comparison of the experimental data with the theoretical. A theoretical analysis was made for the MFI-1A impeller at a weight flow of 13.0 pounds per second in reference 1, and the values obtained are included on some of the figures.

Static pressure. - The experimental static-pressure ratios along the shroud of the MFI-1A impeller and the theoretical static-pressure ratios of the MFI-1 impeller (as computed in reference 1) are presented in figure 9. The high theoretical static-pressure ratios at the impeller inlet result from the assumption of perfect guidance of the fluid by the blades; that is, the direction of the mass weighted average flow is the same as the direction of the blade camber line. If the angle of entry is such that the fluid approaches the driving face of the blades with a positive angle of attack, the sudden turning required by perfect guidance results in instantaneous energy addition. In the experimental case, perfect guidance was not expected. The agreement of the static-pressure ratios near the impeller outlet at the design speed (1400 ft/sec) and peak efficiency (weight flow of 14.3 lb/sec, see fig. 9(a)) indicated that the increase in blade height was not too small in this region; however, it is possible that the increase in area due to increased blade height resulted in excessive boundary-layer build-ups throughout the impeller, which produced the agreement near the outlet, and that closer agreement with higher over-all efficiency may be obtained by reducing the blade height.

Relative velocity. - The computed relative velocity along the shroud, based on experimental static pressures at a speed of 1400 feet per second and experimental weight flows of 14.3 and 13.4 pounds per second is presented in figure 10. In computing the velocity, an estimated internal relative efficiency of 0.90 was used. The value of 0.90 was selected on the basis of the over-all efficiency of these operating points (0.83) and the internal and over-all efficiency measurements presented in reference 3. Theoretical mean velocities along the shroud are included

in figure 10. The lack of agreement between the computed and the theoretical velocities at the inlet may be due to the assumption of perfect guidance of the fluid by the blades and the difficulty encountered in obtaining an accurate theoretical solution in regions of mixed subsonic and supersonic flows. The high computed velocities midway through the impeller may be due to losses caused by the high angles of attack at the inlet and from boundary-layer build-up in the regions of adverse velocity gradients.

Angle of attack. - The angle of attack is defined as the angle between the flow direction of the air at the inlet and the blade camber line, the flow directed at the driving face of the blade being positive. From the analysis of reference 1 it was concluded that for this impeller the angle of attack as determined from the inlet-axial-velocity distribution for flow through the hub-shroud annulus (for the dummy hub) should differ little from the angle of attack for the rotating impeller. Figure 11 shows the variation in the axial velocity as obtained by means of surveys 3/4 inch upstream of the inlet for both the nonrotating dummy hub and the rotating impeller at the weight flow corresponding to peak pressure ratio at an equivalent speed of 1100 feet per second (highest weight flow at which data could be obtained with the dummy hub). The fair agreement shown and the trend are typical of those obtained at other speeds. A comparison of the experimental and theoretical angle of attack at design speed is shown in figure 12. Calculations indicate that approximately 1° of the 5° difference at the mean blade height is caused by the difference in flow rates, 13.0 and 13.4 pounds per second.

Surveys to determine the inlet angles of attack across the passage at the weight flows corresponding to peak pressure ratio were made at two other equivalent speeds, 900 and 1100 feet per second. The results of these surveys, along with the data obtained at 1400 feet per second, are presented in figure 13. The large positive angles of attack near the hub are present at all three speeds.

Maximum flow. - Static-pressure measurements along the shroud for varying back pressure at the outlet indicated that choking took place well inside the impeller at all speeds and moved toward the outlet with decreasing speed. This trend is in agreement with the theoretical analysis for the MFI-1 impeller. The increasing disagreement between the theoretical maximum weight flow for the MFI-1 impeller and the experimental maximum weight flow for the MFI-1A impeller as the speed is decreased (fig. 14) indicates that the allowance for viscous effects was too great for the lower speeds; this is to be expected inasmuch as the pressure gradient from blade to blade (blade loading) decreases with

2567

decreasing speed. Decreasing the blade loading in turn decreases the velocity gradient on the blade trailing face and thus reduces both boundary-layer build-up on the blade trailing face and secondary flow losses. The variations in viscous losses make an accurate prediction of maximum weight flow very difficult when choking occurs at points other than near the inlet. At speeds above 1150 feet per second, the maximum (choke) flow obtained experimentally is 6 to 7 percent higher than that obtained in the theoretical analysis (fig. 14). Theoretically, choking occurred very near the inlet at these speeds and, since no allowance was made for viscous effects in this region, the experimental weight flows would be expected to be lower than the theoretical. This discrepancy may have been caused by negative angles of attack near the shroud at the maximum weight flow-condition. Negative angles indicate that the angle between the relative air flow and the axial direction is less than the angle between the blades and the axial direction. This smaller angle, in combination with the staggered blade row, provides a larger through-flow area at the inlet. Inasmuch as the major portion of the mass flow is passed in the part of the inlet annulus near the shroud, the increase in weight flow resulting from this negative angle of attack could account for the difference obtained.

Slip factor. - The variations of experimental and theoretical slip factors with weight flow, at the design equivalent speed of 1400 feet per second, are presented in figure 15. In computation of the theoretical slip factor, perfect guidance of the fluid by the blades was assumed. In all cases, the slip factors increase as the weight flow is decreased. This increase is a result of backward-curved blades which cause the tangential component of the relative velocity to be in a direction opposite to that of wheel rotation. With a decrease in weight flow, this component is decreased and a higher slip factor results. Thus, with backward-curved impeller blades, it is necessary that the actual outlet velocities equal the theoretical in order to present an accurate comparison of the slip factors. The velocities at the outlet as computed from the experimental data (fig. 10) agree with the theoretical velocities at the outlet of the MFI-1 impeller. The experimental slip factor is a maximum of 0.05 lower than the theoretical slip factor for the MFI-1 impeller. This disagreement may be attributed to the blade loading at the outlet.

With backward-curved impeller blades the effect of splitter blades upon slip factor may be opposite to that normally expected with straight blades. Splitter blades normally tend to raise the slip factor by providing better guidance of the air at the outlet. However, the addition of the splitter blades will reduce the flow area. This reduction in flow area will raise the outlet velocity which, for backward-curved blades, will tend to decrease the slip factor.

SUMMARY OF RESULTS

An investigation of the performance characteristics of a mixed-flow impeller produced the following results:

1. The peak pressure ratio and the maximum adiabatic efficiency at the design equivalent speed of 1400 feet per second were 4.00 and 0.83, respectively. The efficiency over the greater part of the flow range at equivalent speeds from 900 feet per second to design speed (1400 ft/sec) was higher than 0.80.
2. At design speed, the arbitrary increase in blade height near the impeller outlet was not too small to allow for the decrease in the effective flow area caused by viscous effects. At lower speeds, the increase was too large.
3. Theoretically, choking occurred very near the inlet at design speed and the ability of the impeller to pass 6 to 7 percent more mass flow at this speed than was theoretically predicted was probably due to negative angles of attack which increased the flow area at the inlet. When choking occurs at points other than near the inlet, variations in viscous losses make an accurate prediction of maximum weight flow very difficult.
4. The experimental slip factor was a maximum of 0.05 lower at design speed than the theoretical slip factor which was based on perfect guidance of the air by the blades.

Lewis Flight Propulsion Laboratory
National Advisory Committee for Aeronautics
Cleveland, Ohio

REFERENCES

1. Osborn, Walter M., and Hamrick, Joseph T.: Design and Test of Mixed-Flow Impellers. I - Aerodynamic Design and Procedure. NACA RM E52E05, 1952.
2. Ginsburg, Ambrose, Johnsen, Irving A., and Redlitz, Alfred C.: Determination of Centrifugal-Compressor Performance on Basis of Static-Pressure Measurements in Vaneless Diffuser. NACA TN 1880, 1949.
3. Prian, Vasily D., and Michel, Donald J.: An Analysis of Flow in Rotating Passage of Large Radial-Inlet Centrifugal Compressor at Tip Speed of 700 Feet Per Second. NACA TN 2584, 1951.

TABLE I - GEOMETRIC COORDINATES OF MFI-1 AND MFI-1A IMPELLERS^a

Axial depth z (in.)	Blade thickness at hub (in.)	Blade thickness at mean line, MFI-1 (in.)	Blade thickness at shroud, MFI-1A (in.)	Hub radius (in.)	Mean-line radius, MFI-1 (in.)	Shroud radius, MFI-1 (in.)	Shroud radius, MFI-1A (in.)	Angle ϕ (b)	Angle ϕ' (b)
0	0.062	0.022	0.022	1.678	3.210	4.725	4.725	0°	-----
.200	.065	.024	.024	1.695	3.252	4.736	4.763	3°24'	-----
.400	.090	.048	.048	1.718	3.308	4.758	4.792	6°41'	-----
.600	.165	.122	.084	1.752	3.384	4.789	4.819	9°46'	-----
.800	.237	.193	.121	1.801	3.490	4.823	4.863	12°40'	-----
1.000	.260	.260	.192	1.864	3.619	4.868	4.915	15°06'	-----
1.400	.298	.296	.236	2.050	3.900	4.973	5.040	18°38'	-----
1.800	.288	.288	.235	2.380	4.180	5.098	5.200	20°54'	-----
2.200	.272	.272	.223	2.985	4.448	5.247	5.380	22°18'	-----
2.600	.264	.264	.218	3.704	4.708	5.417	5.580	23°06'	-----
3.000	.260	.260	.217	4.120	4.964	5.611	5.782	23°29'	-----
3.400	.298	.259	.218	4.476	5.220	5.808	6.006	23°37'	-----
3.625	-----	-----	-----	-----	-----	-----	-----	-----	15°05'
3.800	.291	.257	.218	4.812	5.472	6.005	6.228	23°39'	15°05'
4.200	.283	.252	.214	5.138	5.724	6.203	6.454	23°31'	14°57'
4.600	.267	.240	.203	5.456	5.978	6.399	6.680	23°24'	14°50'
5.000	.244	.220	.185	5.764	6.228	6.598	6.902	23°21'	14°47'
5.400	.208	.186	.152	6.056	6.480	6.795	7.128	23°23'	14°49'
5.800	.147	.128	.095	6.349	6.716	6.992	7.352	23°29'	14°55'
6.200	.060	.044	.044	6.634	6.940	7.190	7.580	23°55'	15°21'
6.310	.025	.010	.010	6.710	7.000	7.247	7.644	24°05'	15°31'

NACA

^a Splitter-blade thickness at hub is 0.120 in. and at shroud 0.060 in.; leading edge is cut back from z = 3.625 in. at hub along line making a 30° angle with radius through z = 3.625 in. (see fig. 1); number of blades, 21; material used for construction of impeller was aluminum alloy (148-T6).

^b See figure 2.

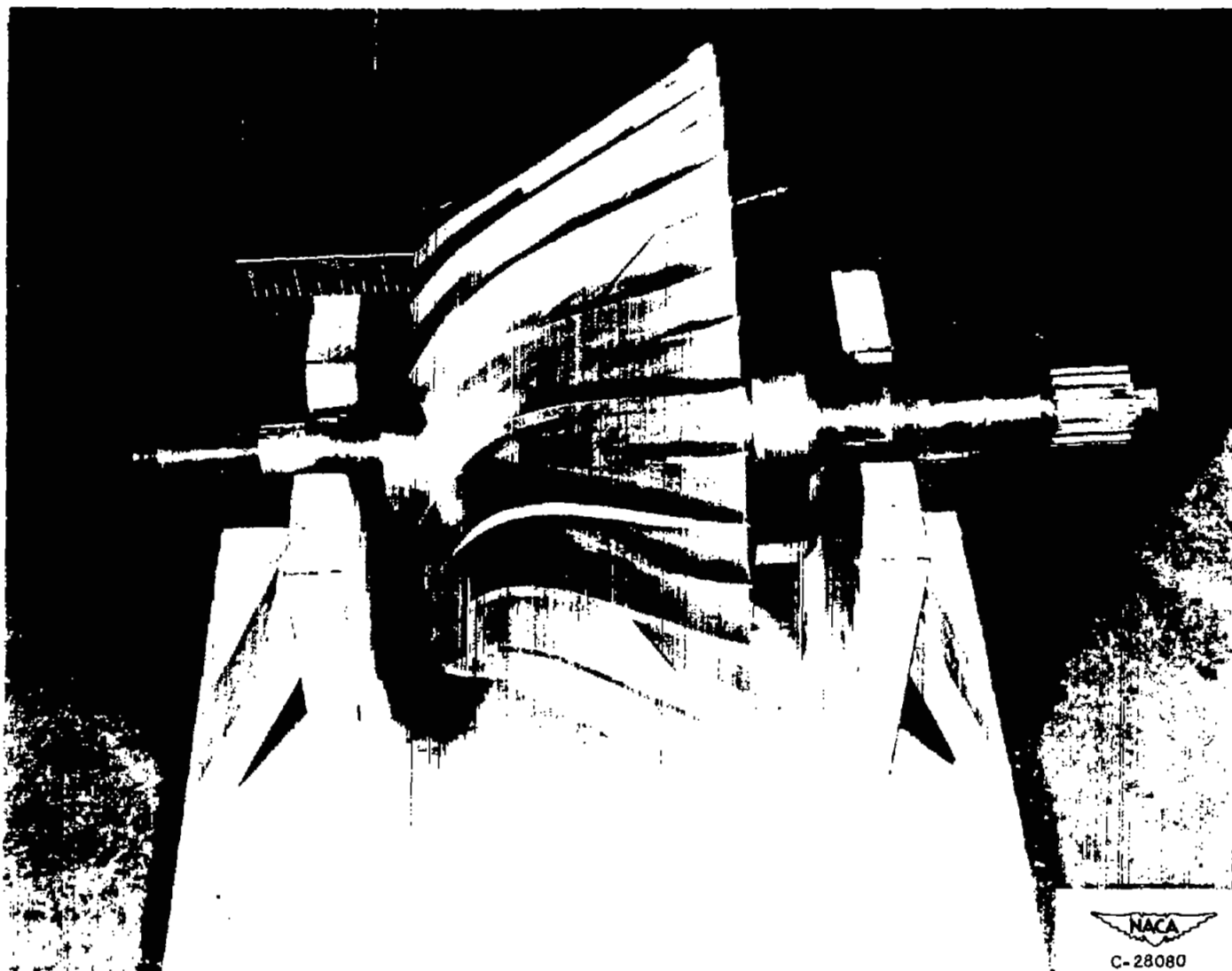


Figure 1. - 14-Inch MFI-1A impeller.

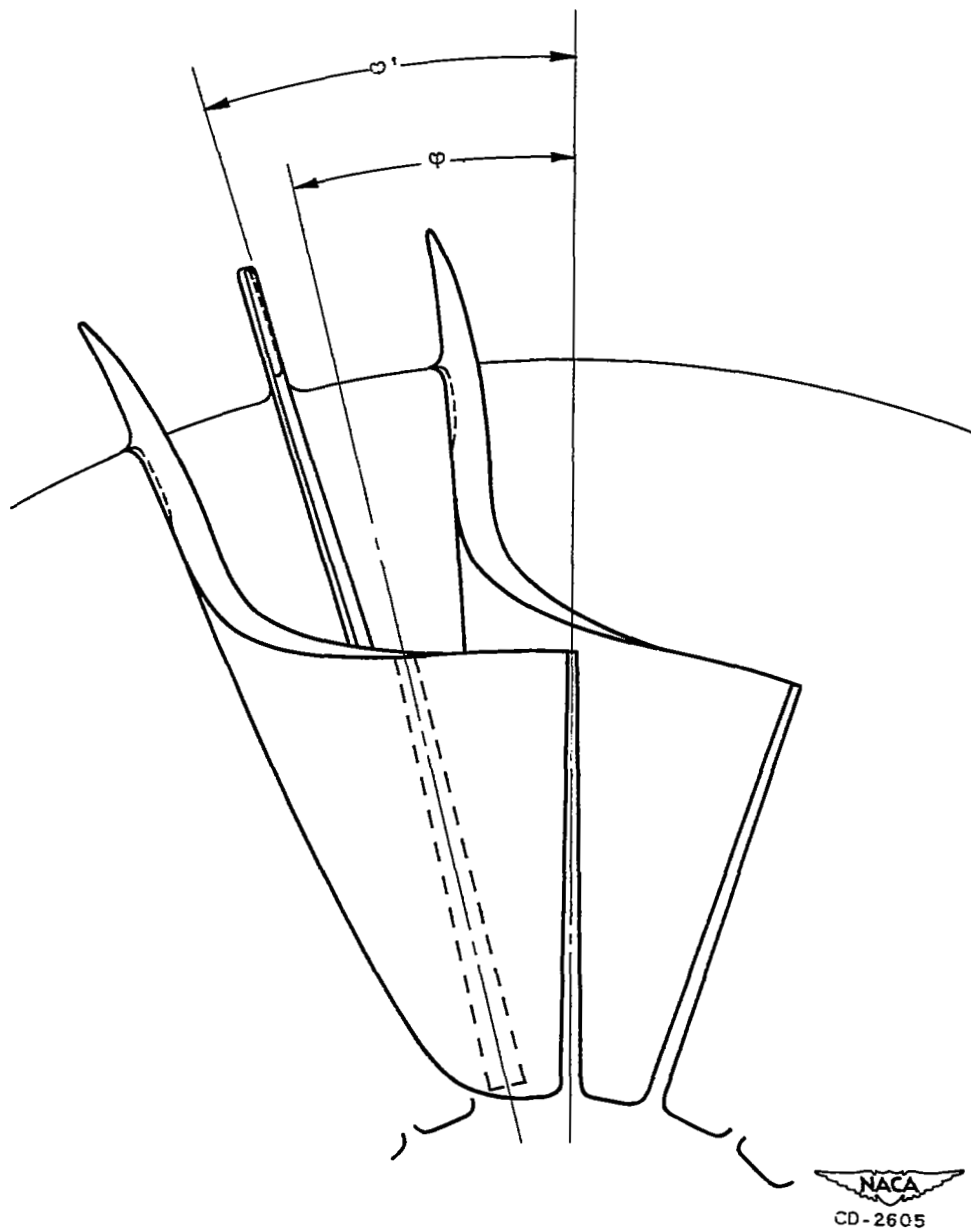


Figure 2. - Front view of MFI-1A impeller showing orientation of angles ϕ and ϕ' .

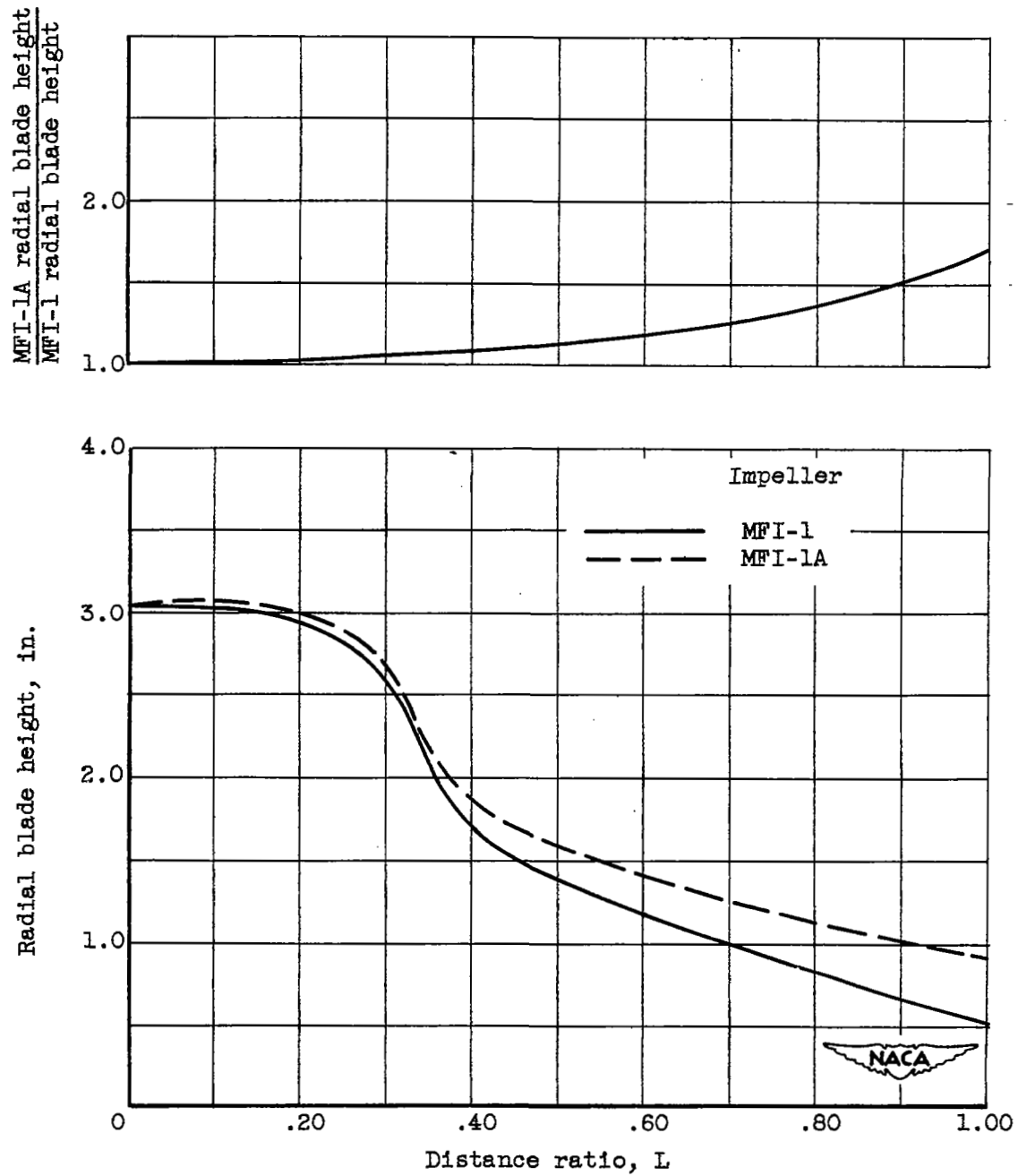


Figure 3. - Radial blade height of MFI-1 and MFI-1A impellers.

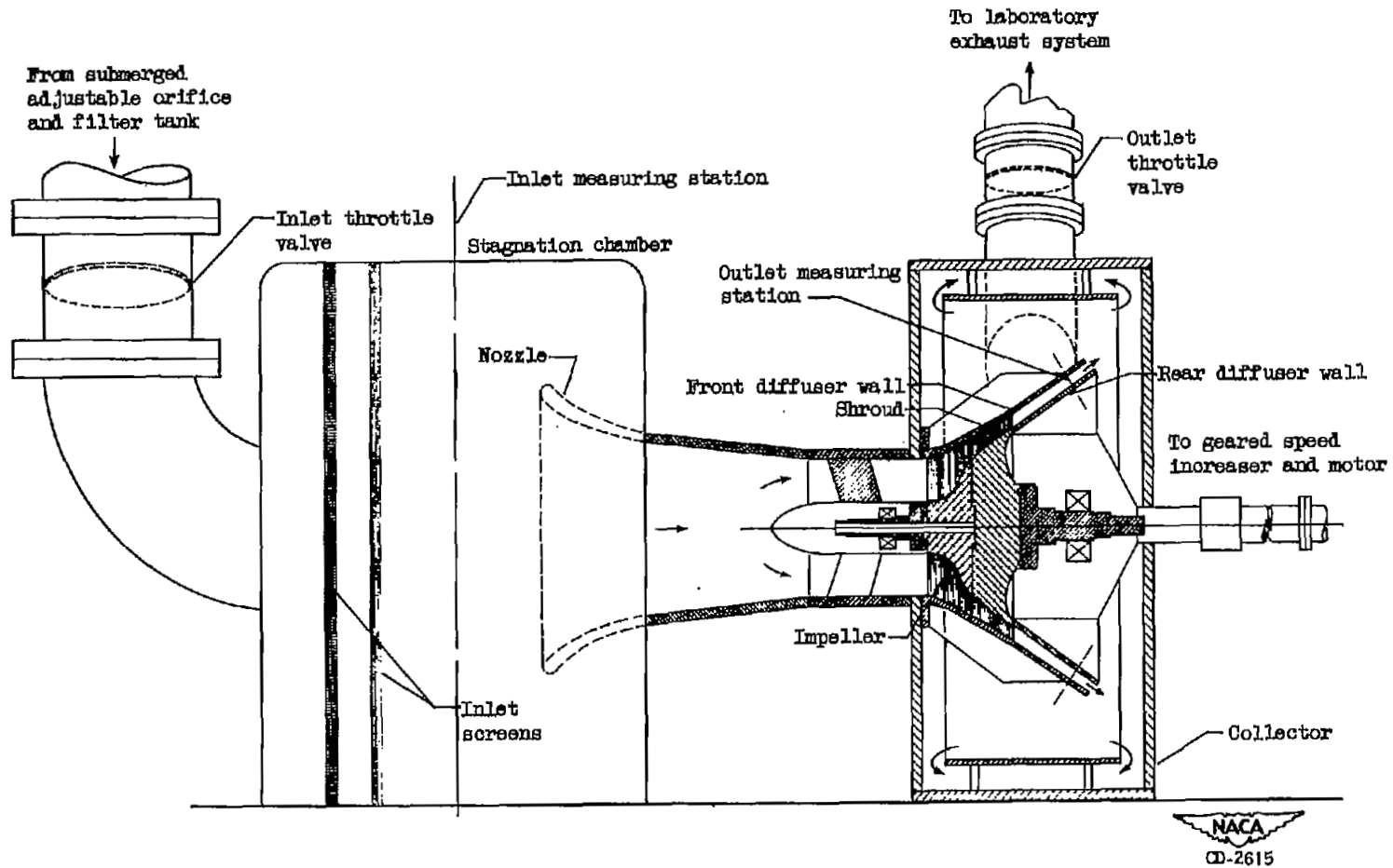


Figure 4. - Experimental setup used in investigation of 14-inch mixed-flow impeller.

(a) Three-dimensional ball-type probe.

(b) Wedge-type static-pressure rake.

(c) Bare-wire spike-type thermocouple rake

(d) Kiel type total-pressure probe.

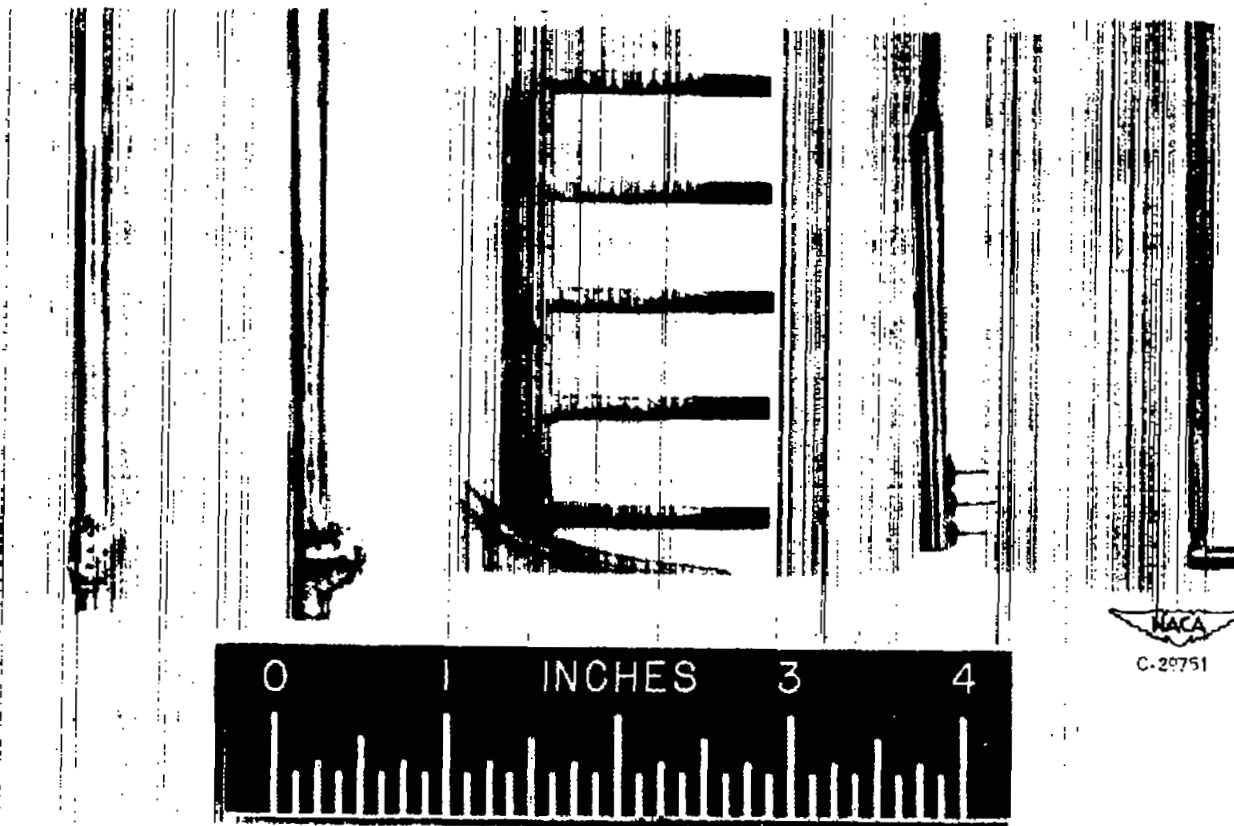


Figure 5. - Instruments used in investigation of MFI-1A Impeller.

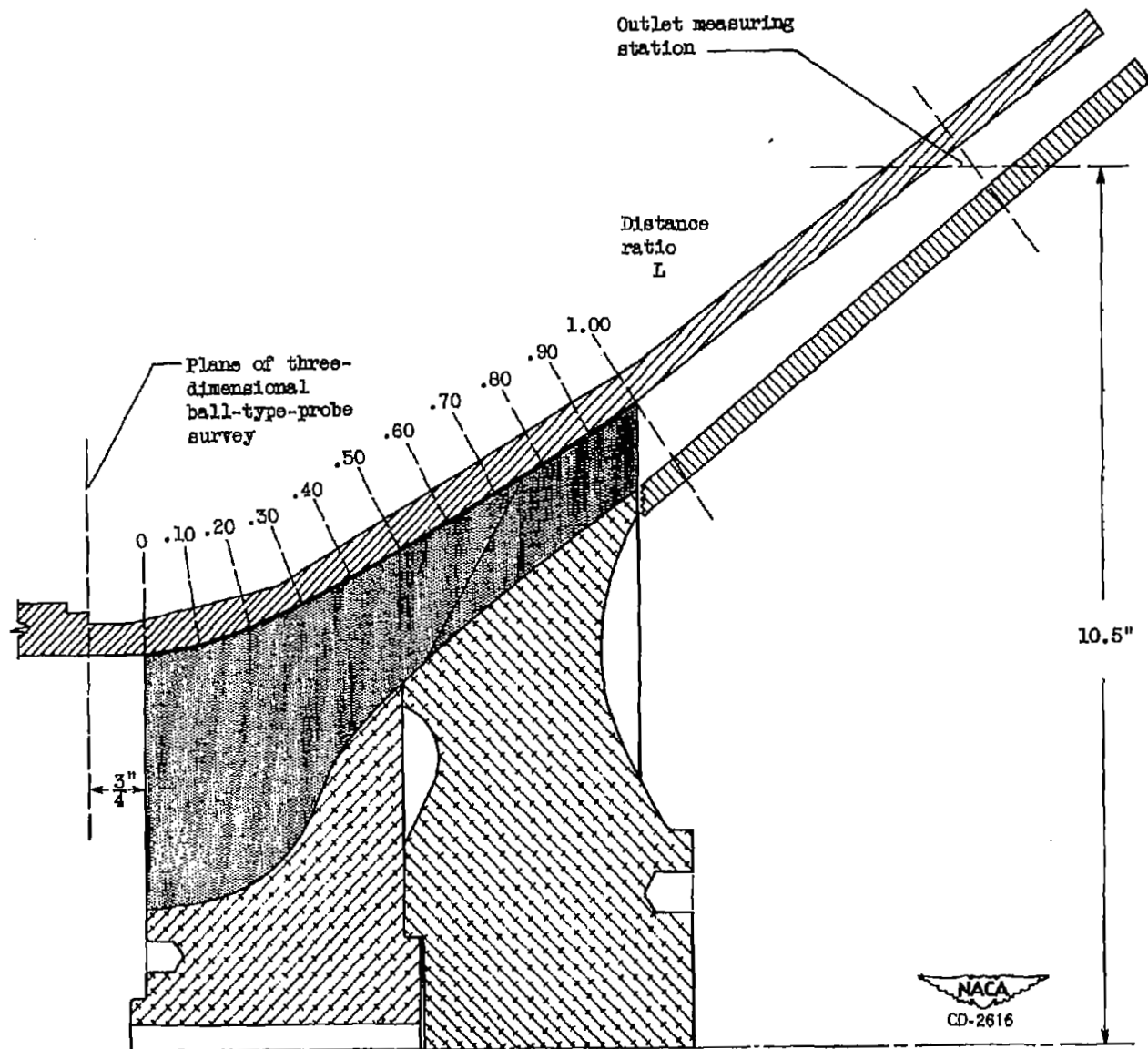


Figure 6. - Instrumentation of experimental setup used in investigation of 14-inch mixed-flow impeller.

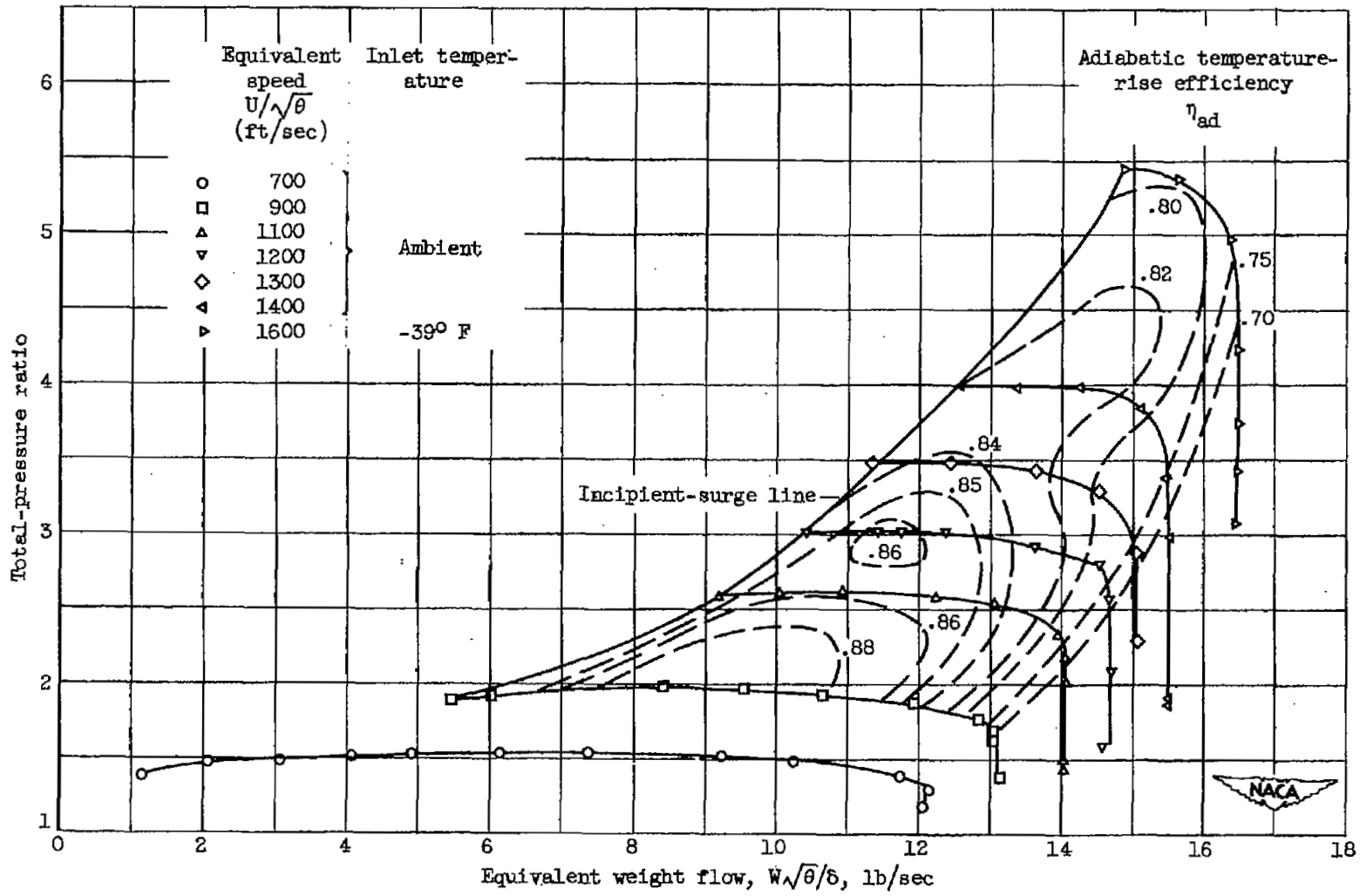


Figure 7. - Over-all performance characteristics of MFI-1A impeller at inlet air pressure of 14 inches of mercury absolute. Ambient inlet air temperature varied from 77° to 82° F.

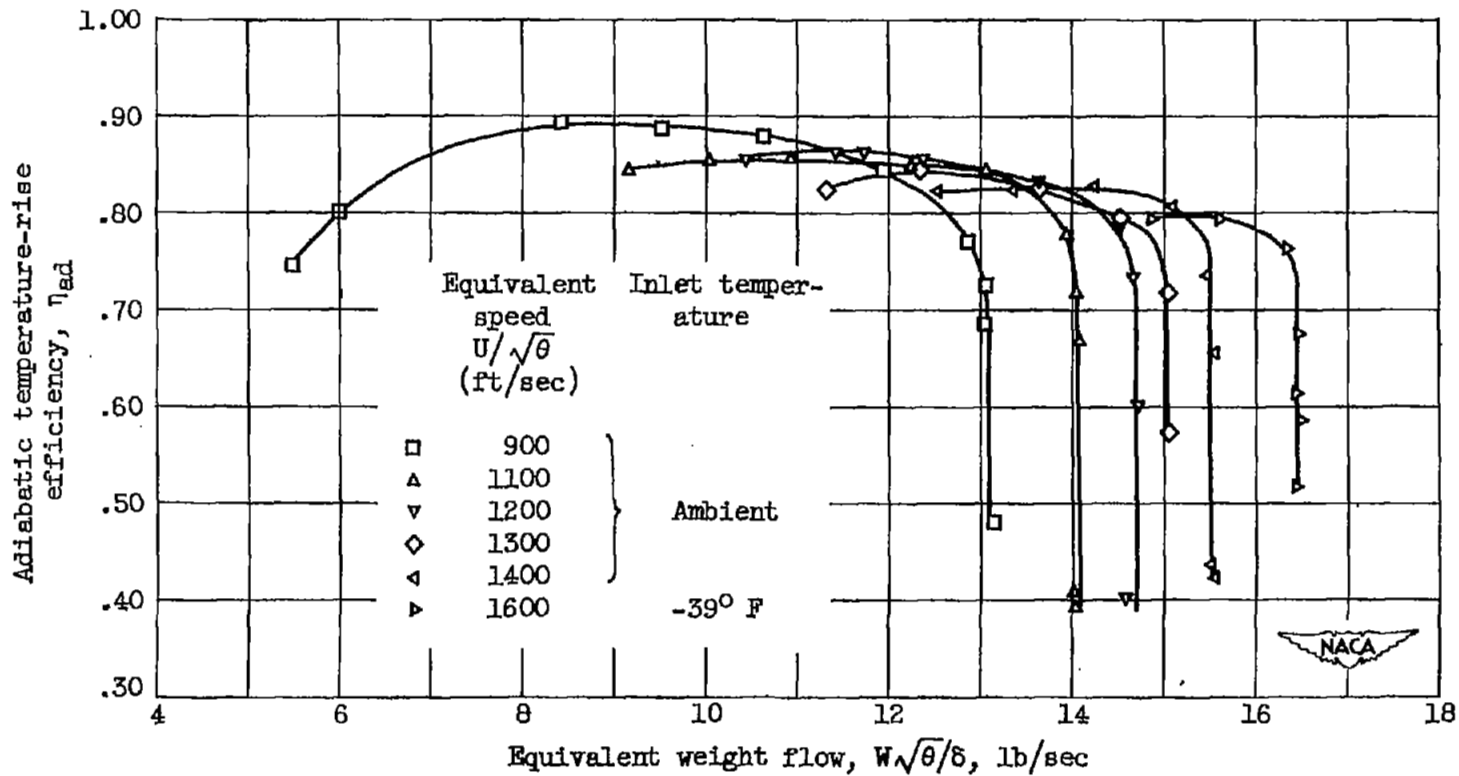
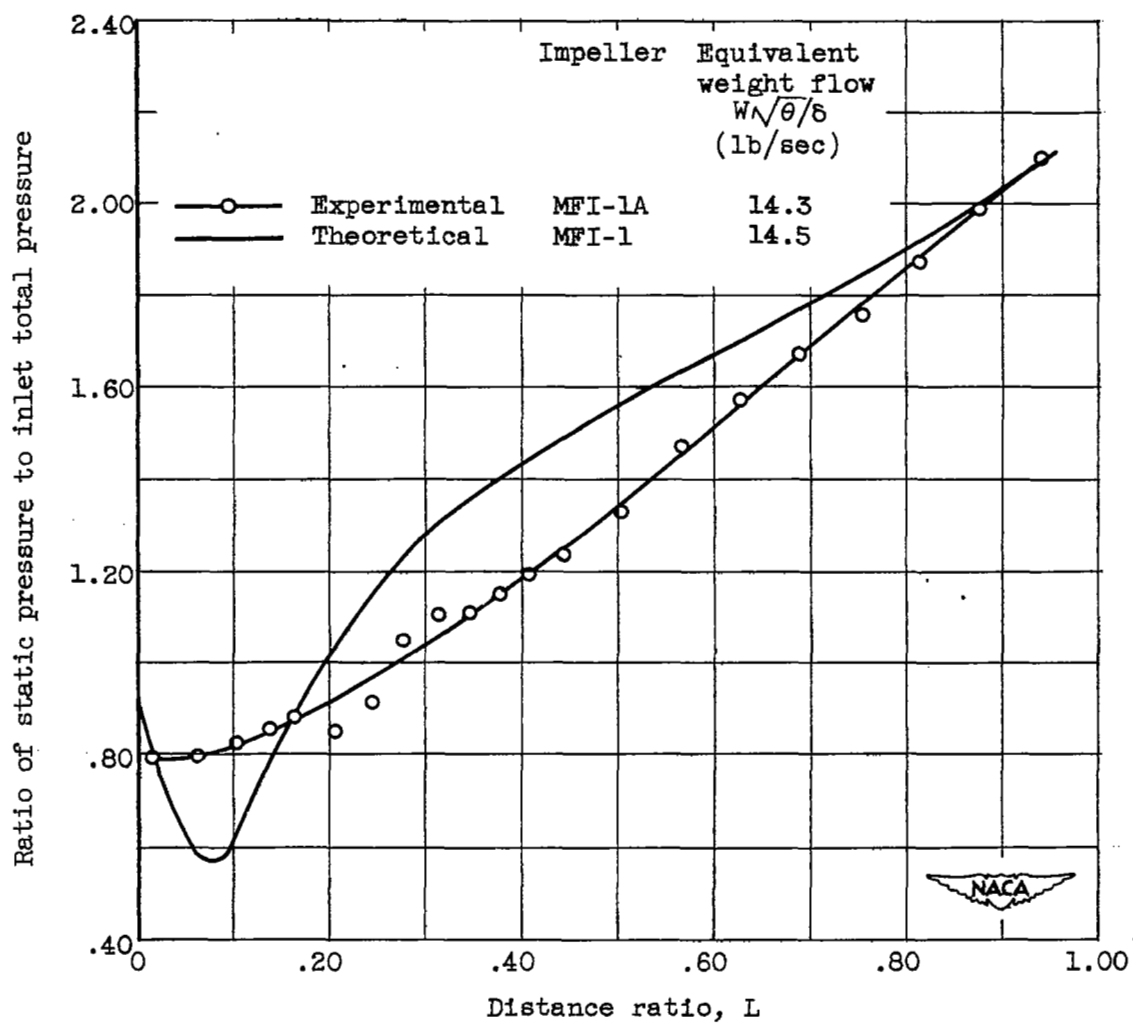
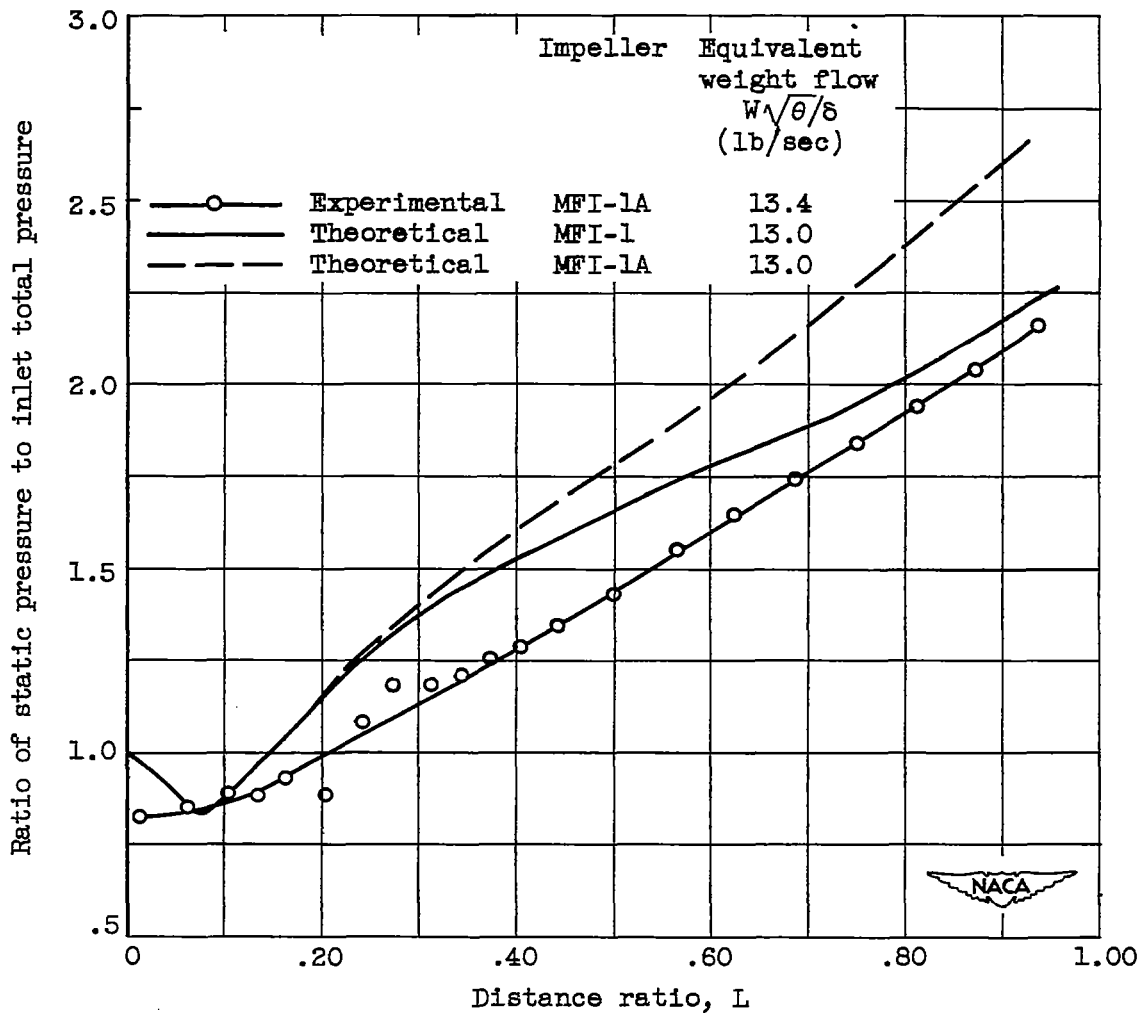


Figure 8. - Variation of adiabatic temperature-rise efficiency with equivalent weight flow at inlet air pressure of 14 inches of mercury absolute. Ambient inlet air temperature varied from 77° to 82° F.



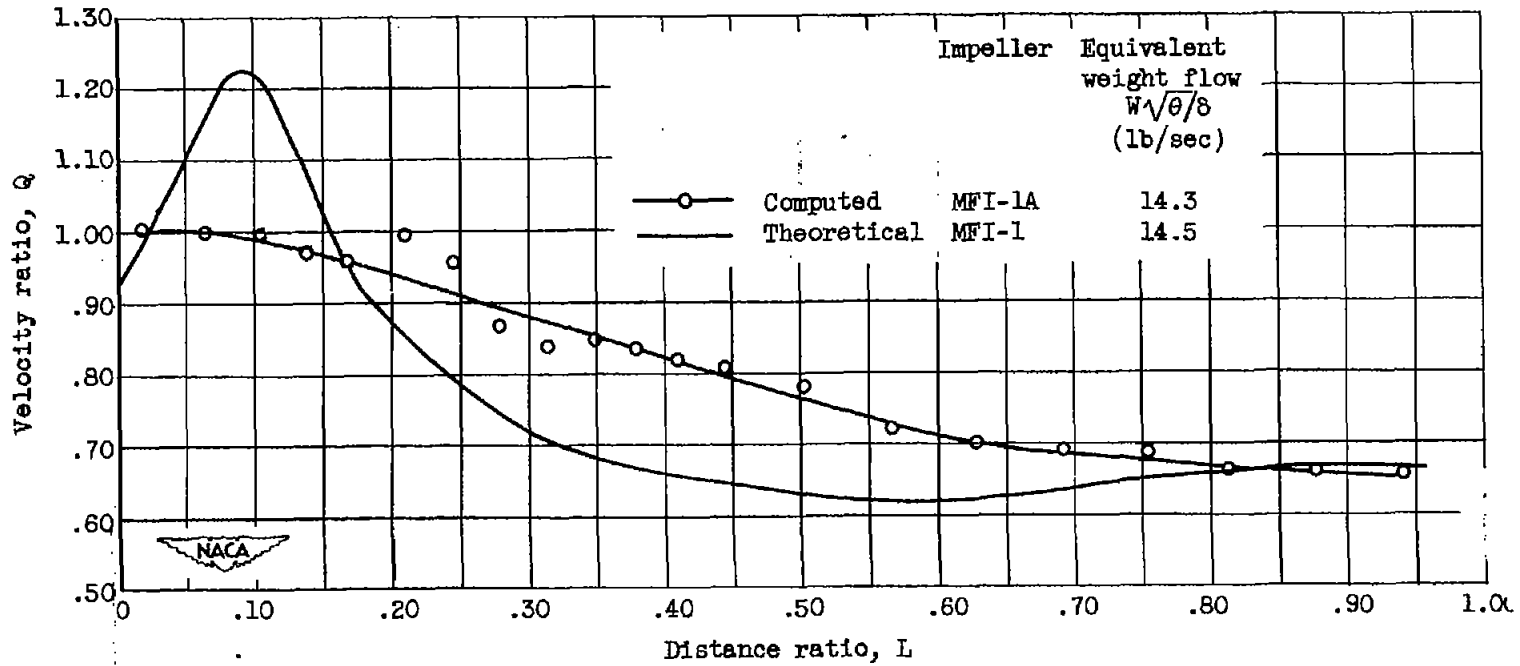
(a) Experimental weight flow, 14.3 pounds per second.

Figure 9. - Static-pressure variation along shroud at equivalent speed of 1400 feet per second.



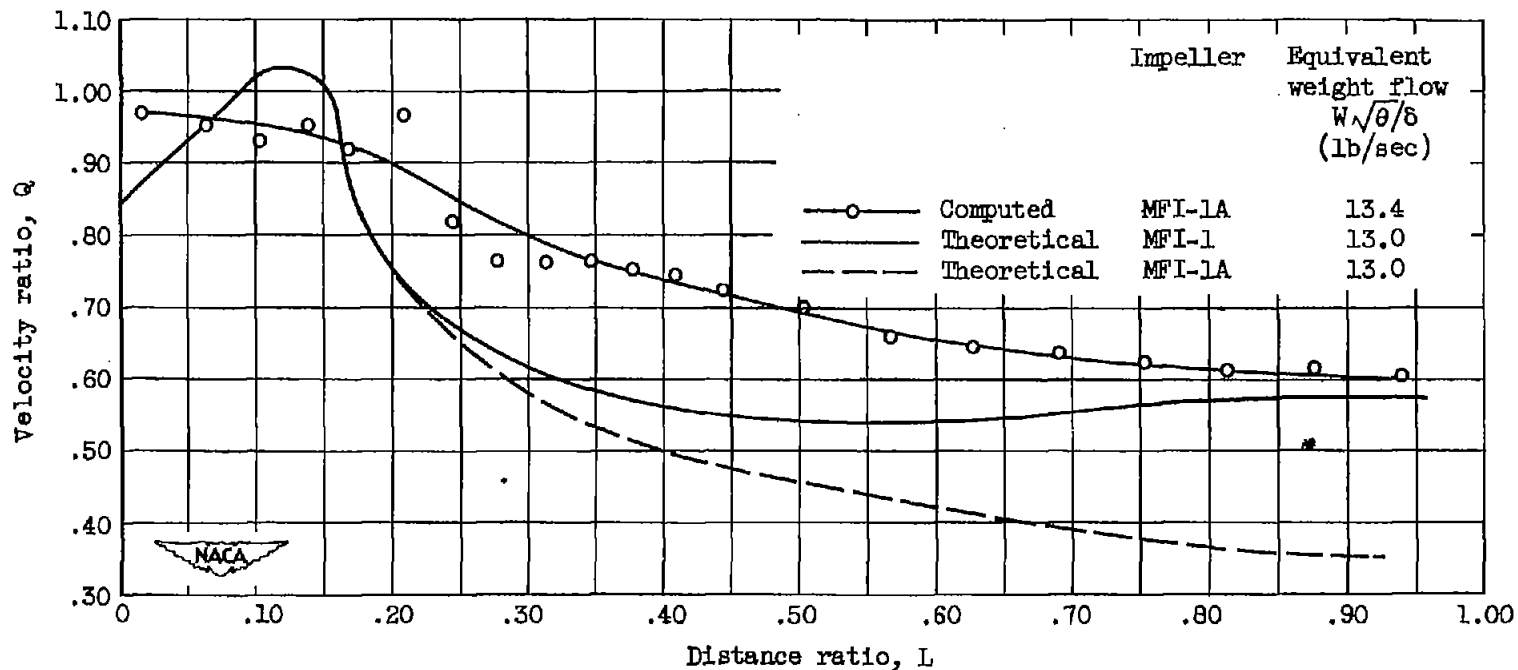
(b) Experimental weight flow, 13.4 pounds per second.

Figure 9. - Concluded. Static-pressure variation along shroud at equivalent speed of 1400 feet per second.



(a) Experimental weight flow, 14.3 pounds per second.

Figure 10. - Mean velocity distribution along shroud at equivalent speed of 1400 feet per second. Computed values are based on experimental static pressures.



(b) Experimental weight flow, 13.4 pounds per second.

Figure 10. - Concluded. Mean velocity distribution along shroud at equivalent speed of 1400 feet per second. Computed values are based on experimental static pressures.

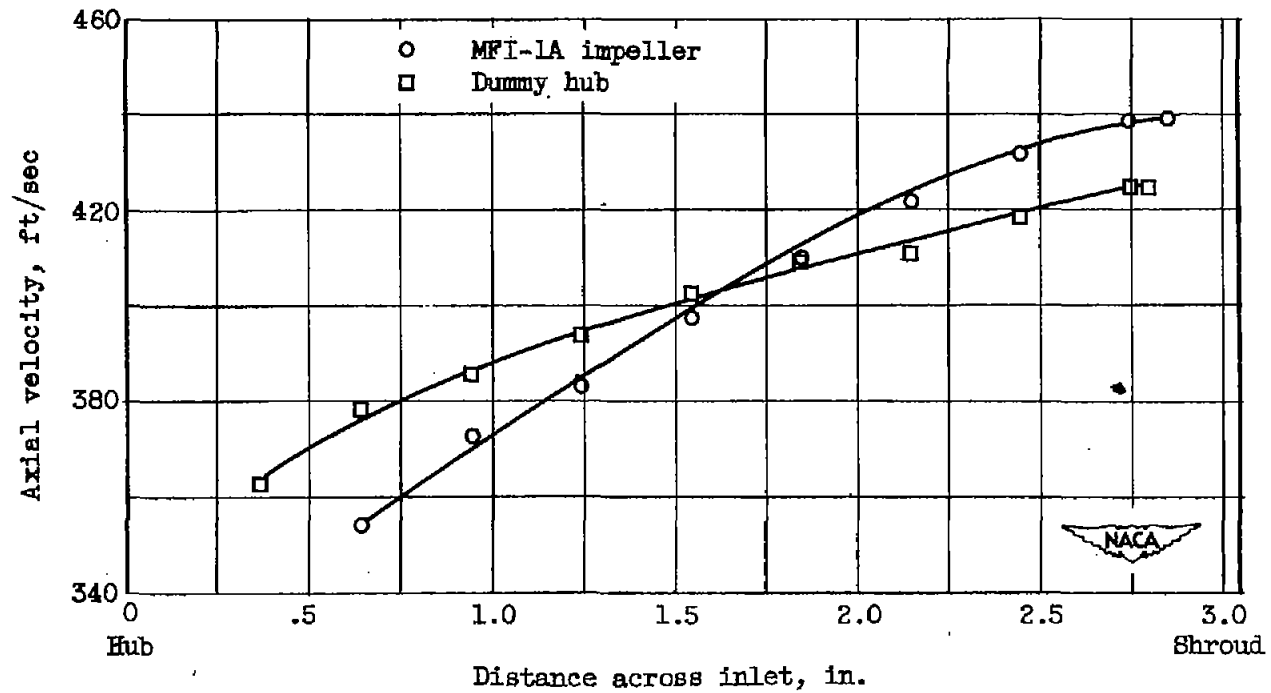


Figure 11. - Axial velocity across inlet section, $3/4$ inch upstream of impeller at equivalent weight flow of 10.8 pounds per second and equivalent speed of 1100 feet per second.

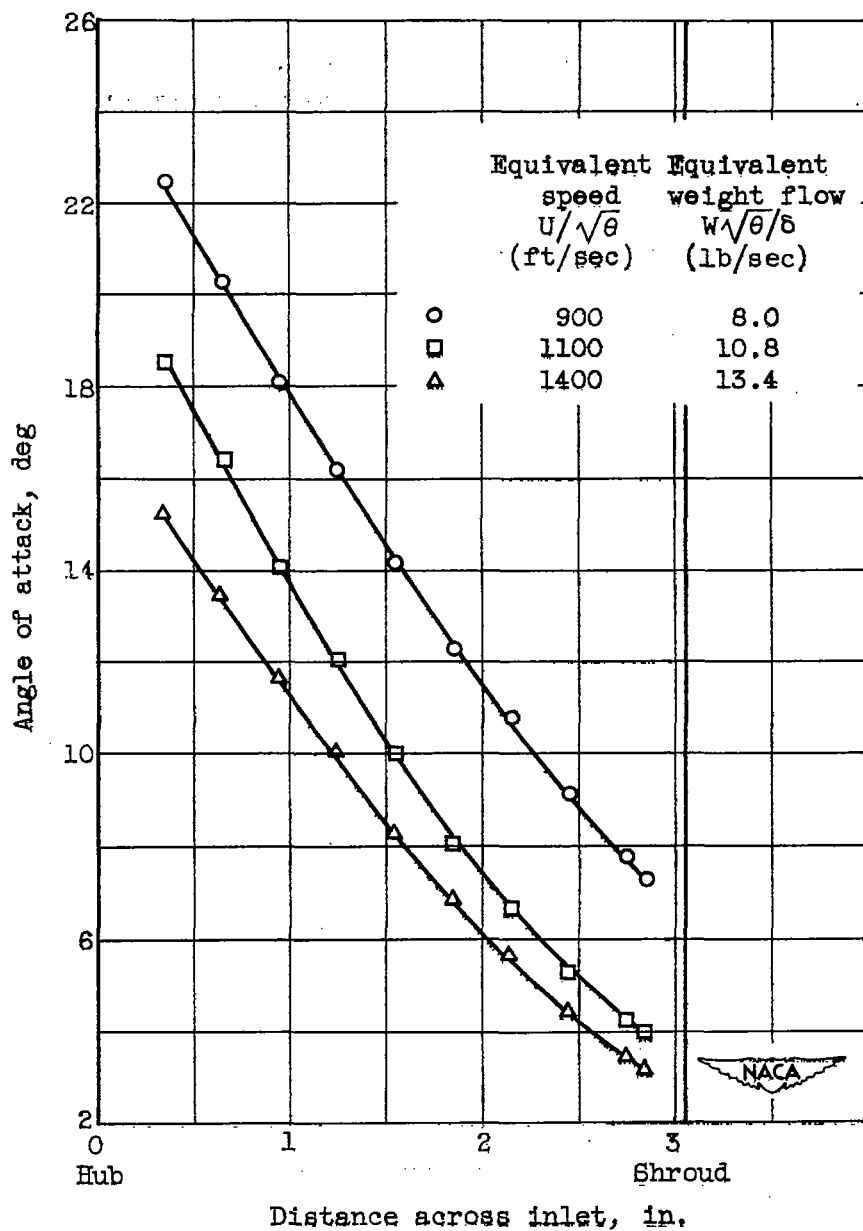


Figure 13. - Angle of attack of MFI-1A at three speeds with weight flows corresponding to peak pressure ratio.

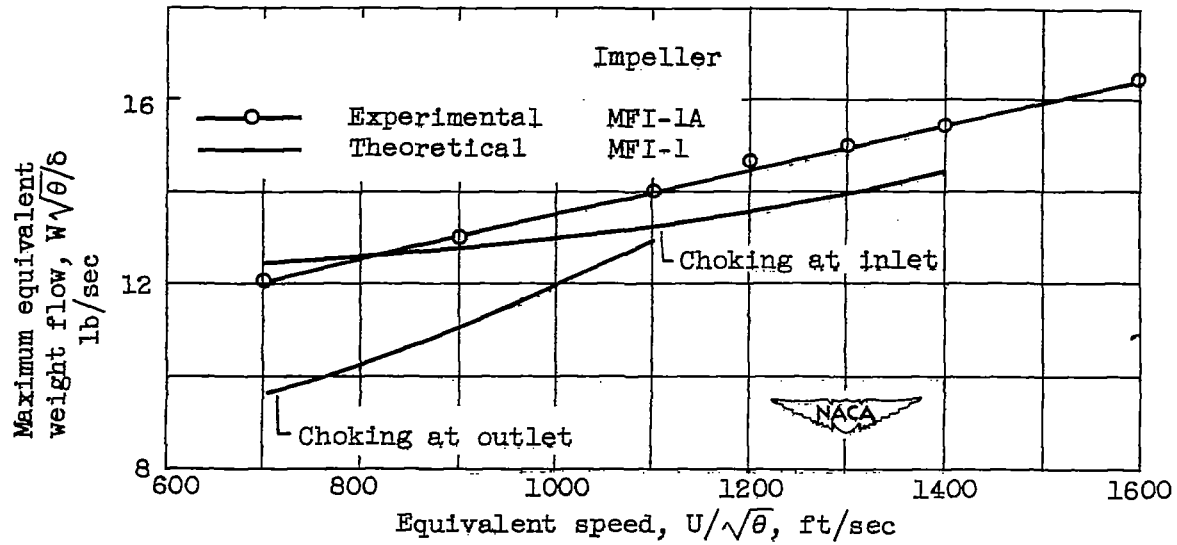


Figure 14. - Experimental and theoretical maximum equivalent weight flows.

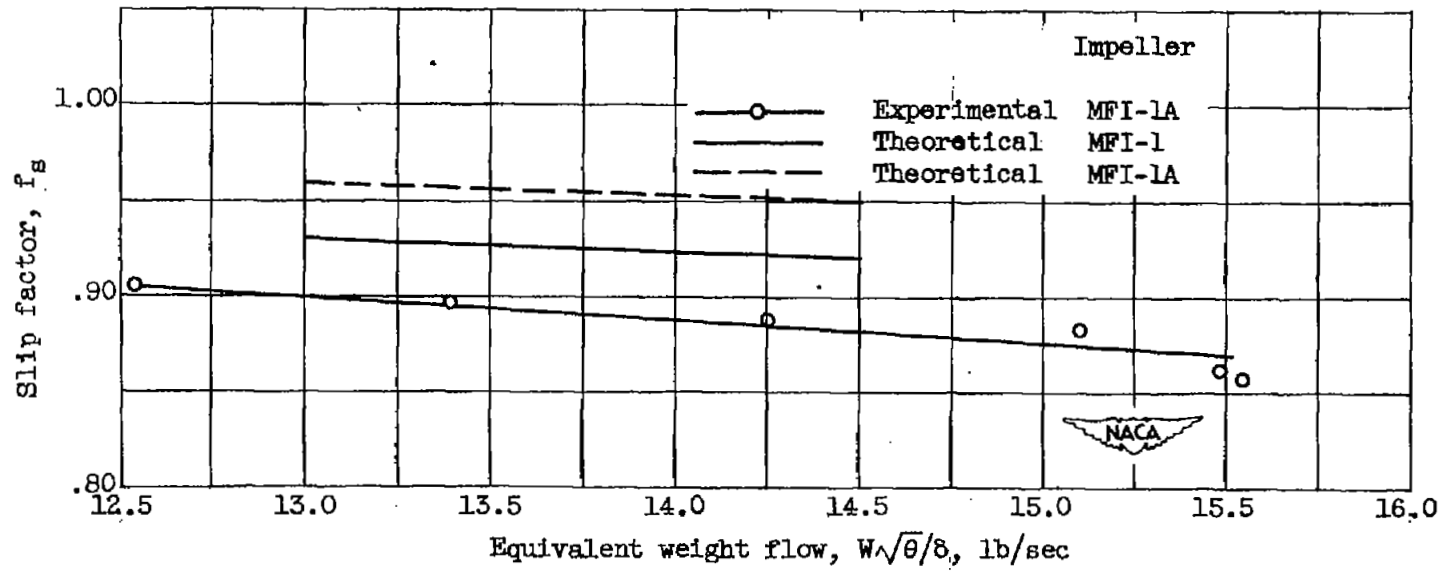
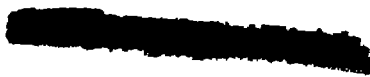


Figure 15. - Experimental and theoretical slip factors at equivalent speed of 1400 feet per second.

SECURITY INFORMATION



NASA Technical Library



3 1176 01435 5979

